Peptide Interaction with a Class I Major Histocompatibility Complex-Encoded Molecule: Allosteric Control of the Ternary Complex Stability†

Dmitry M. Gakamsky,*,‡ Pamela J. Bjorkman,§ and Israel Pecht‡

Department of Immunology, The Weizmann Institute of Science, 76100 Rehovot, Israel, and Division of Biology 156-29, California Institute of Technology, Pasadena, California 91125

Received July 12, 1996; Revised Manuscript Received September 12, 1996⊗

ABSTRACT: Thermodynamics and kinetics of interaction between a soluble class I MHC heterodimer composed of the H-2K^d heavy chain (H) and human $\beta_2$microglobulin (β_2m) with a dansylated peptide series based on residues 147−155 of influenza virus nucleoprotein sequence were studied by means of real-time fluorescence measurements. Peptide−heterodimer binding is a second-order process with specific rates practically independent of peptide structure ($3-5 \times 10^6$ M^{-1} s^{-1}). The ternary complex assembly involves a rate-limiting step of β_2m association with H to yield an unstable heterodimer ($\tau \leq 5$ s, 37 °C). Peptide binding provides a positive feedback enhancing H's affinity for β_2m, thus stabilizing the ternary complex. The latter decays by either peptide or β_2m dissociation. The first-order rate constants of peptide dissociation ($(0.5 \times 10^{-2})-(0.4 \times 10^{-3})$ s^{-1}, 37 °C) depend on their structures and are faster than that of β_2m dissociation. The former process decreases the H affinity for β_2m and induces their dissociation. This dissociation, in turn, drastically lowers H affinity for peptide. Thus, these three components produce a system which is stable as a trimer. This behavior is rationalized by the functional requirements of class I molecules: Peptide structure determines the ternary complex's lifetime, and peptide rebinding on the cell surface is rendered unlikely by the limited stability of the empty heterodimers and the very low peptide affinity of the heavy chains.

Class I major histocompatibility complex-encoded molecules (MHC-I)[1] are an element of a molecular recognition system as they present cellular peptides to cytotoxic T-cells in the framework of the immunological surveillance process. Intracellularly processed peptides are transported to the endoplasmic reticulum (ER) where MHC-I molecules bind them and the MHC-I−peptide complexes are transported to the cell membrane. Thus, an early step in the cascade causing activation of T-cells is binding of antigenic peptides to MHC-I molecules. Hence the assembly rate and the complex stability are important parameters which determine the extent of class I-restricted immune response. Though each individual has only a limited set of MHC-I molecules, these should be able to bind a broad spectrum of peptides with high affinity. Considerable efforts have therefore been made to rationalize the conflict between the requirements for high affinity and a large binding repertoire and understand the ternary complex assembly mechanism.

The three-dimensional structures of several class I−peptide complexes have been determined so far (reviewed by Madden (1995), Stern and Wiley (1994)) and show that the binding site of these molecules has a groovelike shape, created by α_1 and α_2 domains of the heavy chain, which is noncovalently associated with β_2m. Although these domains are polymorphic, there are clusters of highly conserved residues at both ends of the binding groove. In all class I structures determined so far, these conserved residues form hydrogen bonds with the bound peptides' N- and C-termini. These interactions as well as the ∼2.5 nm length of the groove primarily limit the size of binding peptides to 8−10 residues. In addition to these hydrogen bonds, there are some structural features producing preferences for peptide side chains yielding specific binding motifs. For example, in the human HLA-A2.1 molecule, the second residue from the bound peptide N-terminal is usually a leucine and the last one a valine (Hunt et al., 1992; Engelhard et al., 1993; Madden et al., 1991, 1993), whereas for binding to the H-2K^d molecule this second residue should be a tyrosine (Fahnestock et al., 1994; Rotzschke et al., 1990; Falk et al., 1991; Romero et al., 1991; Engelhard, 1994). Thus, the apparent contradiction between the requirements for high binding affinity and a broad peptide repertoire has been rationalized primarily by the sequence-independent binding of the peptide's termini supplemented by side chain interactions with specific pockets of the binding groove (Madden, 1995; Zhang et al., 1992; Stern & Wiley, 1994).

While this provides a qualitative explanation for the above-mentioned contradictory requirements, a more quantitative analysis is still missing. Moreover, the above explanation does not address the role of β_2m, and more generally, why is the class I molecule composed of noncovalently associated heavy and light chains? At the same time there is ample evidence supporting an active role of both β_2m and the peptide in assembly and stability of the ternary complex (Rock et al., 1991; Elliott et al., 1991; Parker et al., 1992;

†This study is part of a collaborative Lower Saxony−Israeli Research Project supported by a grant provided by the Ministry for Science and Culture of Lower Saxony, FRG.

* Corresponding author. Phone: 972-8-9342551. Fax: 972-8-9465264. E-mail: lidima@wis.weizmann.ac.il.

‡The Weizmann Institute of Science.

§ California Institute of Technology.

⊗ Abstract published in *Advance ACS Abstracts,* November 1, 1996.

[1] Abbreviations: MHC, major histocompatibility complex; ET, energy transfer; ER, endoplasmic reticulum; β_2m, β_2-microglobulin; H, heavy chain; L, β_2m; P, peptide; dansylaziridine, [[5-(dimethylamino)-naphthalen-1-yl]sulfonyl]aziridine.

S0006-2960(96)01707-2 CCC: $12.00

Solheim et al., 1995; Smith et al., 1994; Catipovic et al., 1994). Hence considerable efforts were made to resolve the peptide binding mechanism and determine parameters controlling the ternary complex stability. While most of the equilibrium binding studies were interpreted to reflect a single population of binding sites (Olsen et al., 1994; Cerundolo et al., 1991; Matsumura et al., 1992), some proposed the existence of two populations with distinct affinities (Boyd et al., 1992). Conflicting reports have also appeared concerning the role of β_2m in peptide binding: While some observed no effect of excess β_2m on the binding rate (Boyd et al., 1992), others found it increased the binding rate at 37 °C (Matsumura et al., 1992; Olsen et al., 1994). In addition, the equilibrium dissociation constant calculated on the basis of kinetic experiments as the k_{off}/k_{on} ratio corresponded only to the lower affinity sites (Boyd et al., 1992). The above results show that a rigorous analysis of the peptide binding mechanism, preferably by new experimental approaches, is required.

Recent progress in the production of a peptide free form of a soluble recombinant H-2K^d heterodimer (Fahnestock et al., 1992) made it an optimal system for application of a sensitive real-time binding assay. A method based on measuring nonradiative energy transfer from the protein's intrinsic tryptophans to dansyl-labeled peptides in the complex has now been employed (Pecht et al., 1971). Here we present results of kinetic and thermodynamic measurements of peptide binding to the soluble H-2K^d. A quantitative model of the ternary complex assembly based on these results is presented and discussed.

MATERIALS AND METHODS

Reagents and Cells. Purification of secreted K^d−human β_2m heterodimers from transfected CHO cell line, denaturation and removal of endogenous peptides and the reassembly of empty H-2K^d heterodimers have been described in detail elsewhere (Fahnestock et al., 1992). Human β_2m was used instead of its mouse counterpart because higher yields of K^d−human β_2m heterodimers compared to empty K^d−murine β_2m heterodimers are obtained (Fahnestock et al., 1994).

Human β_2m was purchased from Sigma and used without further purification. Dansylaziridine ([[5-(dimethylamino)-naphthalen-1-yl]sulfonyl]aziridine) was purchased from Molecular Probes.

The H-2K^d-restricted peptide NP1 from influenza virus nucleoprotein (amino acid residues 147−155; TYQRTRALV) as well as its derivatives NP19 (TY**C**RTRALV), NP20 (TYQ**C**TRALV), NP21 (TYQR**C**RALV), NP22 (TYQRT**C**ALV), and NP23 (TYQRTR**C**LV) were synthesized by automated solid phase methodology on an Applied Biosystems Model 432A synthesizer using the manufacturer's standard Fmoc protocols. Peptides NP19−NP23 differ from NP1 by sequential substitution of residues 3, 4, 5, 6, or 7 by cysteine. As was previously shown (Fahnestock et al., 1994), these substitutions of a single residue have a relatively limited effect of the peptide binding affinity.

The substituted cysteine in peptides NP19−NP23 was dansylated to yield the respective derivatives (dNP19−dNP23) by the following protocol: 0.3 mL of 10-fold molar excess of dansylaziridine in dimethylformamide was added to 1 mL of peptide solutions (3 mg/mL) in 0.1 M bicarbonate buffer, pH 8.2, and allowed to react for 2 h at room temperature in the dark. The labeled peptides were purified by HPLC. Concentrations of peptides and proteins were determined spectrophotometrically using the extinction coefficient of tyrosine (1.42×10^3 M^{-1} cm^{-1} at 274 nm) (Wetlaufer, 1962) for nondansylated peptides or the extinction coefficient of dansyl (4.57×10^3 M^{-1} cm^{-1} at 350 nm) (Parker, 1968) for the dansylated ones. Extinction coefficients of H-2K^d and β_2m were calculated as 10.1×10^4 and 2.1×10^4 M^{-1} cm^{-1} at 280 nm based on the extinction coefficient of tryptophan and tyrosine. All experiments were carried out in 20 mM TRIS buffer, pH 7.5.

Fluorescence Measurements. Fluorescence spectra corrected for spectral sensitivity were recorded on a Perkin-Elmer MPF-44a spectrofluorimeter with the spectral slits of 6 nm. Titrations and binding kinetics were carried out on a PTI spectrofluorimeter with a single-photon-counting registration system. The sample holder was thermostated with an accuracy of ±0.5 °C. An excitation wavelength of 290 nm (slit width 8 nm) and an emission wavelength from 490 to 530 nm (slit width 16 nm) were used.

Peptide affinity and kinetics of the ternary complex formation were investigated by monitoring the nonradiative energy transfer from intrinsic H-2K^d tryptophans to the dansyl of the bound peptide (Pecht et al., 1971) which allows directly measuring the time course of the reaction. Moreover, this protocol has several important advantages in comparison with monitoring either ligand-induced quenching of the receptor's tryptophan fluorescence or change in the probe's emission (e.g., quantum yield or shift in fluorescence spectrum) induced upon ligand binding. The first is limited by the multiplicity of tryptophan residues (H-2K^d contains 13 tryptophans) causing a maximal specific quenching of the fluorescence upon peptide binding which does not exceed 10%. The second suffers from the contribution of free ligand fluorescence. The presently employed method significantly circumvents the latter problem and takes advantage of the large number of tryptophans present in the H-2K^d molecule, several of which are located in the vicinity of the peptide binding site and participate in energy transfer to dansyl. This further increases the method's sensitivity and allows the use of very dilute samples. In addition, the tryptophan absorption band (270−300 nm) is situated in a minimum between the first and second absorption bands of the dansyl. This allows monitoring specifically peptide binding even when a significant fraction of it is free. For a typical equilibrium titration, different concentrations of peptides were added to 10 aliquots (140 μL) of 0.2 μM H-2K^d and 4 μM excess of β_2m and allowed to equilibrate for 2 h before measurements at 20 °C. The concentration of bound peptides was calculated from the area under the energy transfer band.

Peptide binding kinetics were studied after addition of a small amount (1−3 μL) of one solution (usually heterodimer) to 140 μL of another solution (usually peptide) by a micrometric syringe (Hamilton). Peptide dissociation from the ternary complex was induced by the addition of a large excess of the nondansylated NP1 peptide which blocks the rebinding of the dissociated peptide. The experiments were carried out in a 4 × 4 mm magnetically stirred, quartz optical cuvette.

Data Processing. A Global Analysis program, designed by Dr. A. A. Goldin, was used for processing the observed real-time kinetics. The program provides a nonlinear fit to an arbitrary model which in our case was a sum of exponentials with a background. The program allows

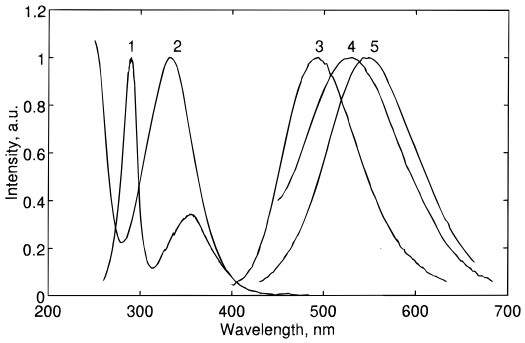

FIGURE 1: Steady-state spectroscopy of dansylated peptides. Excitation (monitored at 550 nm) (curve 2) and emission (excited at 335 nm) (curve 5) spectra of 3 μM dNP21 peptide solution in TRIS buffer (curve 2). An additional excitation band at 285 nm is observed for the ternary complex with all the dansylated peptides due to the nonradiative energy transfer from intrinsic tryptophans of H-2K^d molecule to dansyl, as illustrated here by the excitation spectrum of 2 μM H-2K^d−dNP21 complex (curve 1) (emission monitored at 490 nm). Emission spectra of dansylated peptides−H-2K^d complex as a function of peptide structure: dNP21 (curve 3), dNP20 (curve 4). All the spectra were monitored in 20 mM TRIS buffer, pH 7.5, at 20 °C.

simultaneous processing of several sets of experimental kinetics with linked parameters and an exhaustive search option for estimating the accuracy of the obtained parameters.

RESULTS

Equilibrium Binding Titrations. The fluorescence emission spectrum of the dNP21 in 20 mM TRIS buffer, pH 7.5, at 20 °C exhibits a maximum at 550 nm (Figure 1, curve 5) which was shifted to the blue upon binding to H-2K^d (curves 3, 4). The maximal spectral shift of about 60 nm was observed for bound dNP21 and dNP1, while the shifts for the other peptides were of only 20−25 nm.

A typical example of the fluorescence excitation spectra for one of the dansylated peptides (dNP19) in buffer is shown in Figure 1 (curve 2). Binding of peptide to H-2K^d produced an additional excitation band with a maximum at 285 nm which is a result of the nonradiative energy transfer (ET) from the heterodimer's tryptophans to the peptide dansyl residue (curve 1). The more effective dansyl excitation by ET from the tryptophans compared with the direct one at the maximum of its long wavelength absorption band (340 nm) is probably a result of an increased transfer efficiency from several of these residues which operate as an "optical amplifier". Monitoring ET at the blue slope of the dansyl fluorescence band (480−500 nm) provided an additional selectivity in registering only the bound peptides. Hence, assembly kinetics of the ternary complex could be followed at nanomolar concentrations even when the free peptide concentration exceeded that of the complex severalfold.

A typical titration is shown in Figure 2 where a set of dansyl excitation spectra of the K^d−dNP21 complex was monitored at 490 nm as increasing dNP21 concentrations were added to H-2K^d. Saturation binding curves were calculated presenting the area under the band in the excitation spectrum which represents the energy transfer from tryptophans to dansyl as a function of peptide concentration (Figure 2, inset a). The binding was also found to be a function of both the empty heterodimer and β_2m concentrations where the latter was increased from 0.1 to 4 μM. Incubation of 0.1 μM heterodimer (equimolar concentrations of H and β_2m) with 0.02−0.5 μM dNP21 for 2 h at 20 °C

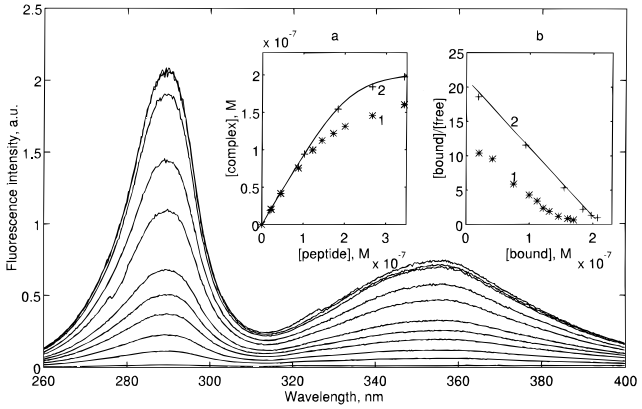

FIGURE 2: Equilibrium titrations of 0.22 μM H-2K^d with dNP21. A set of dansyl excitation spectra (t = 20 °C, λ_{em} = 490 nm) was recorded at increasing peptide concentrations. Inset: Effect of β_2m concentration on apparent affinity of H-2K^d heterodimer for the peptide. Equilibrium binding curves (a) present the area under the energy transfer bands as a function of peptide concentration (0.01−0.3 μM) in the presence of excess β_2m (above the equimolar ratio of heavy chain/β_2m of the heterodimer); [β_2m] = 1 μM (*, curve 1), [β_2m] = 4 μM (+, curve 2). (b) Scatchard plots of the binding data.

Table 1: Activation Parameters and Equilibrium Dissociation Constants of the Peptide−H-2K^d Interaction[a]

peptide	K_d (nM)[b]	K_d^{kin} (nM)[c]	$\Delta H_{on}^{\ddagger}$ (kcal/M)	$-T\Delta S_{off}^{\ddagger}$ (kcal/M)	$\Delta H_{off}^{\ddagger}$ (kcal/M)
dNP19	0.35 ± 0.05	0.4 ± 0.10	18.3 ± 1.5	4.9 ± 2.0	17.5 ± 2.0
dNP20	0.20 ± 0.05	0.5 ± 0.10	19.0 ± 1.5	3.6 ± 1.5	18.9 ± 1.5
dNP21	12.0 ± 3.0	13.0 ± 3.0	18.7 ± 1.5	1.1 ± 1.5	19.0 ± 1.5
dNP22	1.8 ± 0.4	1.7 ± 0.60	20.9 ± 1.5	1.7 ± 1.5	19.8 ± 1.5
dNP23	0.25 ± 0.05	0.3 ± 0.10	19.4 ± 2.0	2.5 ± 2.0	17.5 ± 2.0

[a] Equilibrium dissociation constants were determined from both equilibrium titrations and kinetic experiments. [b] Dissociation constants K_d were measured at 20 °C with 4 μM excess of β_2m. [c] Dissociation constants K_d^{kin} were calculated as a ratio of the peptide dissociation and binding rate constants at 20 °C.

yielded a rather small amount of H-2K^d−dNP21 complexes (not shown). A saturation curve of 0.22 μM H-2K^d in the presence of excess 1 μM β_2m and its Scatchard analysis are shown in insets a and b of Figure 2 (curves 1). Under these experimental conditions, a curved Scatchard plot is observed. However, a titration at a higher β_2m concentration (4 μM) increased the concentrations of produced ternary complexes (inset a, curve 2) and yielded a linear Scatchard plot (inset b, curve 2). Further increase in β_2m concentration did not affect the binding.

The equilibrium dissociation constants of the studied peptide series were therefore determined in the presence of 4 μM excess β_2m and are presented in Table 1. One can see that under these conditions all peptides exhibit affinities that are 1−2 orders of magnitude higher than those of their nondansylated counterparts reported earlier (Fahnestock et al., 1994), the reason most probably being the presence of excess of β_2m in the presently studied samples and not the derivatization with dansyl.

Kinetics of Peptide Binding. In order to investigate the mechanism of peptide binding as well as the role of H−β_2m interaction in this process, we studied the time course of binding at different concentrations of heterodimer and peptides, with or without an excess of β_2m. Usually, the observed time course of binding was biphasic. This is illustrated by an experiment (Figure 3a) carried out with a significant excess of the peptide ([dNP22] = 3 μM, [H-2K^d]

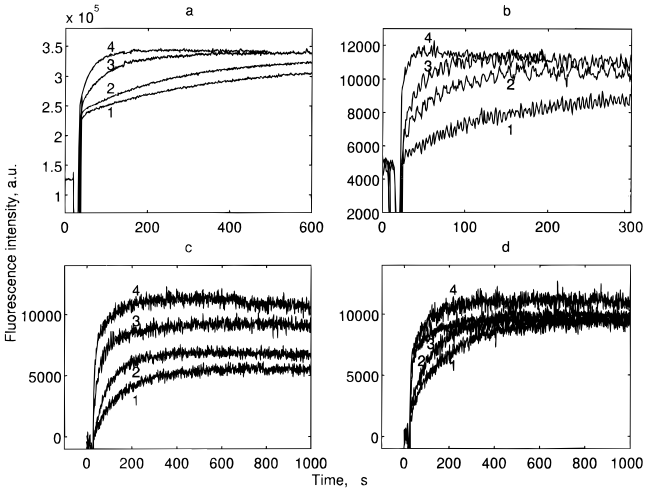

FIGURE 3: Time course of dNP22 binding to H-2K^d monitored by the nonradiative energy transfer from the heterodimer intrinsic tryptophans to the dansyl group carried on the bound peptide as a function of temperature (excitation 290 nm, emission 510 nm): (a) slow phase, [H-2K^d] = 0.4 μM, [dNP22] = 3 μM, [β_2m] = 1 μM, t = 3 °C (1), 5 °C (2), 19 °C (3), 34 °C (4); (b) fast phase, [H-2K^d] = 0.06 μM, [dNP22] = 0.5 μM, t = 0 °C (1), 5 °C (2), 10 °C (3), 15 °C (4). Time course of dNP21 binding to H-2K^d in the absence (c) or presence (d) of 4 μM β_2m excess at t = 10 °C; 0.5 μL of a stock solution (H-2K^d, 2 μM; β_2m, 3 μM) was diluted into 140 μL of solution of the following dNP21 concentrations: 0.05 μM (1), 0.1 μM (2), 0.2 μM (3), and 0.8 μM (4).

Table 2: Time and Rate Constants of the Fast Binding Phase of dNP21 and dNP22 to the H-2K^d Molecule as a Function of Peptide Concentration[a]

[H-2K^d] (μM)	[dNP21] (μM)	[dNP22] (μM)	τ (s)	k_2 (10^5 s^{-1} M^{-1})	T (°C)
0.014	0.075		113 ± 10	1.1 ± 0.2	10
0.014	0.15		67 ± 8	1.0 ± 0.2	10
0.014	0.3		21 ± 5	1.6 ± 0.3	10
0.014	0.6		13 ± 4	1.3 ± 0.3	10
0.014	1.2		8 ± 3	1.1 ± 0.4	10
0.02		0.14	147 ± 10	0.49 ± 0.04	0
0.02		0.27	78 ± 7	0.47 ± 0.05	0
0.02		0.54	34 ± 4	0.55 ± 0.06	0

[a] In the experiment 1 μL (dNP21) or 1.5 μL (dNP22) of stock of H-2K^d protein (2 μM heterodimer and 3 mM β_2m) was added into 140 μL of peptide solutions of different concentrations.

= 0.4 μM, [β_2m] = 1 μM) to fulfill conditions of a pseudo-first-order reaction. The fast binding phase could not be resolved in this experiment due to the limiting mixing time (about 3 s in the magnetically stirred cuvette). It could however be resolved at lower concentration of the reactants (e.g., 0.06 μM H-2K^d, 0.5 μM dNP22) (Figure 3b). One can see that the amplitude of the binding kinetics at 15 °C (curve 4) decayed after reaching the maximum (after 75 s). We found that this decay was a result of β_2m dissociation from the ternary complex and could be eliminated by addition of excess β_2m (see Figure 6a,b).

In order to elucidate the significance of these two phases, we studied the binding as a function of peptide and β_2m concentrations. The time constant of the fast phase was independent of β_2m concentration ($\leqslant$5 μM) and decreased linearly with peptide concentration at a constant heterodimer concentration (Table 2). Similarly, the complex formation amplitude depended on peptide concentration (Figure 3c). We repeated the experiments illustrated by Figure 3c with an excess of 4 μM β_2m which did not affect the binding rate constants. However the dependence of the fast phase amplitude on peptide concentration was almost completely eliminated (Figure 3d). Therefore the fast phase is a second-order process assigned to peptide binding to the heterodimer. At constant heterodimer concentration the slow phase was a function of both peptide and β_2m concentrations (Table 3). Being therefore attributed to the complex assembly from H, β_2m, and peptide, the reaction is a consecutive second-order process as depicted below by the kinetic scheme (eqs 1 and 2).

Table 3: Binding Time Constants of the Dansylated Peptide dNP22 to the H-2K^d Molecule as a Function of β_2m and Peptide Concentration, t = 10 °C

[heavy chain] (μM)	[β_{2m}] (μM)	[dNP22] (μM)	τ (s)
0.2	1.2	1.0	383 ± 20
0.2	1.2	3.0	200 ± 15
0.2	1.2	6.0	113 ± 10
0.4	0.4	3.0	340 ± 20
0.4	1.4	3.0	211 ± 15

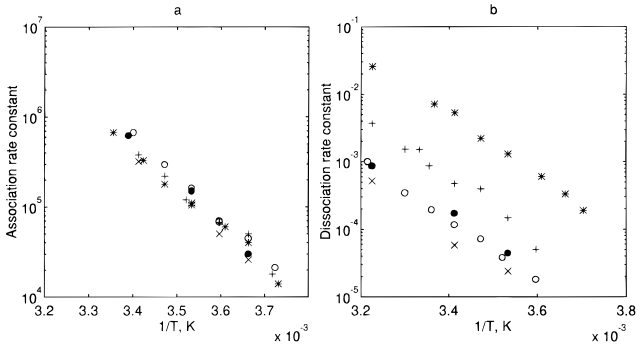

FIGURE 4: Arrhenius plots of the association and dissociation rate constants of H-2K^d complexes with dNP19 (○), dNP20 (×), dNP21 (*), dNP22 (+), and dNP23 (●); 20 mM TRIS solution, pH 7.5.

The temperature dependence of the heterodimer−peptide complex formation kinetics was also studied, and both the fast and slow phases exhibited a similar behavior (Figure 3a,b). The rate constants of the second-order binding process were determined for all peptides in the temperature range of 0−20 °C. The resultant Arrhenius plots are presented in Figure 4a. The temperature dependence was linear for all peptides, having within limits of experimental errors practically the same slopes. The binding rate constants at physiological temperature were calculated by linear extrapolation of the Arrhenius plots to 37 °C as 3−5 × 10^6 M^{-1} s^{-1}.

We found it noteworthy that the contributions of both fast and slow phases to the binding process were rather sensitive to the design of the experimental protocol: Very different patterns were observed in experiments with identical initial concentrations of the reagents depending on the temporal sequence of their mixing. For example, curve 2 in Figure 5 was obtained following dilution of the empty H-2K^d heterodimer from a stock (5 μL of 2 μM heterodimer and 3 μM excess of β_2m) into 135 μL of 0.5 μM dNP22 solution. In contrast, curve 1 was obtained upon first diluting 5 μL of the above stock into 125 μL of buffer and adding the dNP22 (10 μL of 7 μM) after 20 min incubation at 37 °C. The latter protocol eliminated the fast binding phase which was very pronounced when the protein was reacted immediately with the peptide.

Peptide Dissociation Measurements. The peptide dissociation kinetics were studied by adding an excess (50 μM) of competitive nonlabeled peptide, NP1, to H-2K^d-labeled

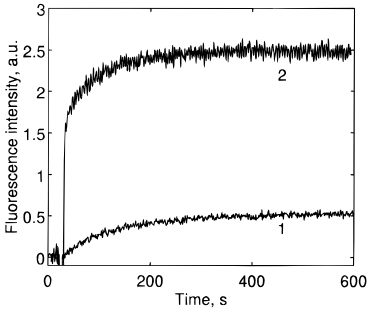

FIGURE 5: Time course of dNP22 binding to H-2K^d monitored by the nonradiative energy transfer (excitation 290 nm, emission 530 nm) as a function of initial experimental conditions at $t = 37$ °C; [H-2K^d] = 0.1 μM, [dNP22] = 0.5 μM, [β_2m] = 0.15 μM: (1) H-2K^d preincubated at 37 °C for 20 min before addition of the peptide, (2) H-2K^d stock solution 20-fold diluted from 2 μM H-2K^d heterodimer + 3 μM excess of β_2m directly into a 0.5 μM dNP22 solution.

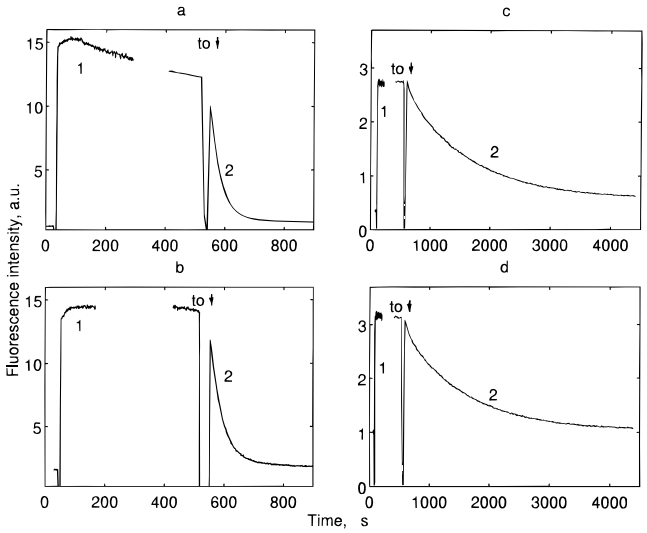

FIGURE 6: Time course of peptide dissociation from H-2K^d complex with different dansylated peptides as a function of β_2m concentration ($t = 37$ °C). The peptide exchange reaction was started by addition of 50 μM of the nonlabeled peptide NP1 to the samples. Peptide complexes were prepared by mixing (a, b) [H-2K^d] = 70 nM, [dNP21] = 2 μM on (c, d) [H-2K^d] = 80 nM, [dNP19] = 0.5 μM; 4 μM excess of β_2m above equimolar ratio of the heterodimer was added in experiments b and d.

peptide complexes. These were prepared by mixing (~0.1 μM) heterodimer with 0.5 μM dansylated peptides in the presence or absence of 4 μM excess of β_2m. It can be seen (Figure 6) that at 37 °C the complexes were produced within a few seconds. Complexes with dNP19, dNP20, dNP22, and dNP23 exhibited no further change in their fluorescence intensity after reaching a maximum during the first 2 min.

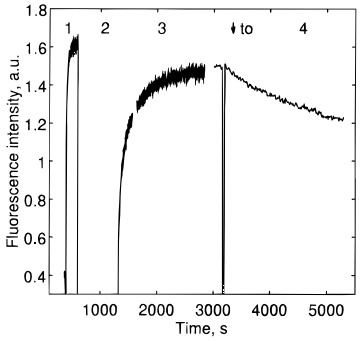

FIGURE 7: Reversibility of H-2K^d−peptide complex assembly and dissociation. [H-2K^d] = 80 nM and [dNP19] = 0.5 μM, $t = 37$ °C, were reacted at the first phase of experiment (1). The produced complex was dissociated by heating at 58 °C for 12.5 min (2). The sample was then cooled back to 37 °C for 2 min, and the fluorescence signal monitored at 530 nm was almost completely (90%) restored during this third phase of the experiment (3). Dissociation of the peptide from the complex was then induced by addition of 50 μM NP1 peptide at the indicated time point (4).

A slow declining phase was however observed for the dNP21 (Figure 6a) and dNP1 (not shown) complexes which was eliminated when the excess of β_2m (4 μM) was present (Figure 6b). The dissociation process induced by addition of a competing, nondansylated peptide did not depend on either β_2m or the initial complex concentrations and exhibited, for all examined peptides, a double-exponential decay pattern. Parameters of the double-exponential fit to this decay curve are listed in Table 4. Complexes with peptides dNP19, dNP20, dNP22, and dNP23 dissociated mainly (70−90%) with a slower rate constant (k_{2f}), whereas dNP21 and dNP1 dissociated primarily with the faster one (k_{1f}). The temperature dependence of the rate constants calculated from the dominant exponential term of the dissociation curve is presented in Figure 4b. Significantly, the slopes of all these plots were practically the same though the dissociation rate constants were quite different.

Assembly Reversibility. Experiments designed in order to study the reversibility of the ternary complex assembly and its thermal stability are illustrated by Figure 7; a solution of the H-2K^d−dNP19 complex was heated at 58 °C for 12 min (phase 2). This thermal treatment caused complete dissociation of the complex. The sample was reequilibrated at 37 °C within ca. 2 min, and the fluorescence signal due to complex formation began being restored. The time course of this restoration was significantly slower (phase 3) than that of its initial formation (phase 1). The reassembled complex exhibited the same dissociation kinetics (phase 4) as that determined for similar ones that did not undergo heating. Reassembly of the complex was however blocked

Table 4: Analysis of Peptide Dissociation Kinetics of the H-2K^d Complex with Different Fluorescently Labeled Peptides[a]

peptide	[β_{2m}] (μM)	α_1 amplitude	k_{1f} (s^{-1})	α_2 amplitude	k_{2f} (s^{-1})
dNP1		0.60 ± 0.10	0.5 ± 0.2	0.40 ± 0.10	(0.9 ± 0.3) × 10^{-1}
dNP19		0.10± 0.04	(0.11 ± 0.02) × 10^{-1}	0.90 ± 0.05	(0.95 ± 0.08) × 10^{-3}
dNP19	3.4	0.09 ± 0.04	(0.14 ± 0.02) × 10^{-1}	0.91 ± 0.05	(1.00 ± 0.06) × 10^{-3}
dNP20		0.10 ± 0.04	(0.17 ± 0.03) × 10^{-1}	0.90 ± 0.10	(0.56 ± 0.04) × 10^{-3}
dNP21	4.2	0.95 ± 0.05	(0.29 ± 0.03) × 10^{-1}	0.05 ± 0.04	(0.43 ± 0.06) × 10^{-2}
dNP21		0.95 ± 0.04	(0.25 ± 0.03) × 10^{-1}	0.05 ± 0.05	(0.50 ± 0.10) × 10^{-2}
dNP22		0.20 ± 0.10	(0.20 ± 0.03) × 10^{-1}	0.80 ± 0.10	(0.43 ± 0.04) × 10^{-2}
dNP23		0.30 ± 0.04	(0.67 ± 0.06) × 10^{-2}	0.70 ± 0.10	(0.83 ± 0.06) × 10^{-3}

[a] Dissociation was induced by addition of 50 μM nonlabeled NP1 peptide; [H-2K^d] = 0.1 μM, $t = 37$ °C. The time course of the complex dissociation was fitted to a following biexponential function: $y(t) = \alpha_1 \exp(-k_{1f}t) + \alpha_2 \exp(-k_{2f}t)$, where $y(t)$ is the fluorescence intensity change (normalized to 1), α_1 and α_2 are the preexponential factors reflecting the fluorescence intensity amplitude, and k_{1f} and k_{2f} are the peptide dissociation rate constants from the unstable (HLP) and stable ({HLP}) conformations (see Discussion).

when 1% of a detergent (Triton X-100) was added to the sample (not shown).

DISCUSSION

Two discrete phases were resolved in the time course of H-2K^d association with all peptides employed in this study (Figures 3, 5). The fast phase was shown to be a second-order process and is attributed to the association of peptides with the heterodimer. The slow phase was found to depend on the concentration of all three reaction partners and therefore is attributed to the complex assembly by a consecutive reaction of the separated heterodimer chains and peptide. Therefore, the biphasic reaction reflects existence of the heterodimer in equilibrium with its dissociated components. The ratio of these two states is a function of the heavy chain and β_2m concentrations. This is illustrated by the dilution-induced dissociation of the empty H-2K^d heterodimer shown in Figure 3c. In this experiment (at 10 °C) the rates of the heterodimer dissociation and peptide binding to it were of the same order of magnitude. Therefore the amount of ternary complexes produced in this reaction by association of the heterodimer and peptide (as reflected by the amplitude of the fast binding phase) was determined by the rate of the heterodimer dissociation and reactant concentrations. As a result we monitored a decrease in the complex production yield upon slowing down the peptide binding rate by decreasing peptide concentration. The ternary complex assembly from the three separated components was much slower under these experimental conditions and did not contribute to the observed reaction. These measurements allow to estimate the empty heterodimer dissociation rate constant. As the reaction amplitude decreased by one-half when the binding time constant was slowed down from 12 s (curve 4) to 60 s (curve 1) upon lowering the peptide concentration, we estimated the dissociation rate of the empty heterodimer to be about $2 \pm 1 \times 10^{-2}$ s^{-1}. At physiological temperature (37 °C) we expect it to be severalfold faster.

The ternary complex assembly may therefore be described by the following reaction scheme where the first step (k_1) represents the heterodimer assembly from the heavy chain (H) and β_2m (L) followed by peptide (P) binding (k_2):

$$\mathrm{H} + \mathrm{L} \underset{k_{-1}}{\overset{k_1}{\rightleftharpoons}} \mathrm{HL} + \mathrm{P} \underset{k_{-2}}{\overset{k_2}{\rightleftharpoons}} \mathrm{HLP} \quad (1)$$

$$\mathrm{H} + \mathrm{P} \underset{k_{-3}}{\overset{k_3}{\rightleftharpoons}} \mathrm{HP} + \mathrm{L} \underset{k_{-4}}{\overset{k_4}{\rightleftharpoons}} \mathrm{HLP} \quad (2)$$

The second route where the heavy chain first binds the peptide (k_3) and then associates with the light chain (k_4) apparently operates only at a high peptide concentration (Table 3). In addition since HP dissociation was fast (unpublished results), the yield of the ternary complex production is strongly determined by β_2m concentration.

The peptide binding experiments (Figure 3) clearly show that the multiple-phase kinetics of peptide binding is a result of the heterodimer's instability. When its dissociation is attenuated by addition of β_2m excess, the equilibrium shifts toward the heterodimer and the reaction amplitude dependence on peptide concentration is eliminated (Figure 3d). Under these experimental conditions, peptide binding to the heterodimer becomes a regular bimolecular process. The observed biphasic binding (Figure 3a) is therefore not a result of the existence of two binding sites with different affinities as has been previously suggested (Boyd et al., 1992) but rather a result of the ternary complex assembly from either the empty heterodimer and peptide or the separated chains and peptide.

A similar manifestation of the heterodimer's limited stability is also evident in the results of experiments illustrated in Figure 5. The fast bimolecular binding phase was observed when stock solution of the heterodimer (where the heterodimer was the dominant component) was directly diluted into a 0.5 μM dNP22 solution. However, this fast phase completely disappeared when the heterodimer was first diluted to the same concentration as in the previous case, yet the peptide was added only after 20 min incubation at 37 °C. Therefore, disappearance of the fast phase is a result of the heterodimer dissociation induced by dilution, and the monitored complex assembly was from its three separated components.

The lability of the heterodimer is thus a result of the limited affinity of the heavy chain and β_2m. The low affinity is not an artifactual result of using a murine H chain−human β_2m hybrid heterodimer, since the K^d−human β_2m heterodimer is slightly more stable than K^d−mouse β_2m heterodimer (Fahnestock et al., 1994). The separated heavy chain and β_2m are sufficiently stable so that we observed an almost complete reversibility of NP19 complex assembly even after being heated to 58 °C (Figure 7). This is in good agreement with results of the previous thermal stability studies (Fahnestock et al., 1992) showing that the H-2K^d−peptide complex exhibits proper refolding even after being heated to 80 °C. In our experiments, the reassembly rate of the ternary complex was slower than that of its original formation since the former proceeded from the separated (and probably partially unfolded) chains of the heterodimer and peptide, whereas the complex production in the experiment's first phase was mainly the result of peptide binding to the heterodimer. Interaction of detergent molecules with dissociated heavy and light chains apparently hinders their reassociation and therefore makes the complex dissociation irreversible. This again is in good agreement with reported earlier results (Matsumura et al., 1992).

Comparison of experiments done with equimolar concentrations of the heavy chain and β_2m with those done using an excess of β_2m show that β_2m concentration does not affect the peptide binding rate constant, k_2, but shifts the equilibrium to the formation of more heterodimers. Therefore, the role of β_2m is in forming the high-affinity sites in agreement with other results showing that peptide binding does not require the concomitant separation of the heavy chain and β_2m (Matsumura et al., 1992). Although β_2m is only indirectly involved in creating the high-affinity binding site, its interaction with the heavy chain most probably changes H conformation. It is known from the protein's sequence and three-dimensional structure that only the α_1 domain lacks the disulfide bridge which is probably required for stability of its active fold (Smith et al., 1994). We suggest that the α_1−β_2m interaction compensates for the absence of the latter disulfide bond and promotes stability of its folding. Although peptide binding does not require β_2m dissociation from the heavy chain and peptide binding to the heterodimer is relatively fast, the binding rate constant is smaller than the lower limit of the diffusion controlled processes by about 1 order of magnitude $3-5 \times 10^6$ M^{-1} s^{-1}. This not only

could be a result of an enthalpic contribution to the activation energy but also might reflect an entropic barrier in the system.

While the bimolecular peptide binding rate constants did not exhibit a marked dependence on the structure of the studied peptides (Figure 4a), the dissociation rate constants did (Figure 4b). This is further illustrated by the Arrhenius plots of the dissociation constants of all studied peptides which were also linear in the temperature range 0−37 °C and had practically the same slopes but differed in intercept values (Table 1).

The dNP20 complex exhibited the slowest dissociation rate constant (0.56×10^{-3} s^{-1} at 37 °C), whereas dNP21 and dNP1 dissociated much faster (0.25×10^{-1} and 0.5 s^{-1} at 37 °C, cf. Table 4). All H-2K^d−peptide complexes except for the least stable ones (NP21 and dNP1) did not show any marked decay without β_2m excess, and only addition of the nonlabeled NP1 peptide induced decay of the fluorescence signal due to the peptide dissociation. The observed slow decay of the dNP21 and dNP1 complexes was found to be a result of β_2m dissociation, since it was essentially eliminated by an excess of β_2m. We did not observe β_2m dissociation from complexes with the other peptides (dNP19, dNP20, dNP22, dNP23), most probably because the process was too slow to be resolved on an examined time scale. Although the ternary complex dissociation can proceed by dissociation of either peptide or β_2m, the peptide dissociation rates are faster and hence determine the complexes' lifetimes. The rate constant of β_2m dissociation from the ternary complexes is significantly slower than that of the empty heterodimer. Even for one of the less stable complexes with dNP21, the rate constant of β_2m dissociation was slower at 37 °C (1×10^{-3} s^{-1}) than that of the empty heterodimer (2×10^{-2} s^{-1}) at 10 °C. Thus, peptide binding stabilizes the ternary complex, and the stabilization is higher the slower the peptide dissociation rate constant.

Peptide dissociation and replacement kinetics were independent of either the complex or added β_2m concentrations and are therefore reflecting a unimolecular process. Surprisingly though, the observed decay functions were biexponential (Table 4). Since all the employed peptides were highly purified, we assign the phase with the smaller amplitude (10−30%) of the more stable ternary complexes (with dNP19, dNP20, dNP22, and dNP23) to the decay of their lower stability conformers. In contrast, the main fraction of the less stable complexes (with dNP21 and dNP1) dissociated very fast, and only a minor fraction decayed at a slower rate, apparently from a more stable conformer. Hence we note that the slower the peptide dissociation rate constant, the higher the relative weight of the longer lived component in the peptide dissociation process. Therefore, peptides of an appropriate structure probably can induce a conformational change in the heavy chain. The probability of such a transition determines the ratio of the long to short decay components of peptide dissociation from the ternary complex.

The conformational transition induced in the heavy chain upon peptide binding increases the heavy chain−β_2m affinity. This increases the stability of the ternary complex to the extent that its lifetime is determined by the peptide dissociation which in turn is a function of its structure. Therefore the above complex assembly scheme is extended by the following step where HLP and {HLP} are the lower and higher stability conformations.

$$\mathrm{HLP} \rightleftarrows \{\mathrm{HLP}\} \qquad (3)$$

The proposed existence of the ternary complex's two conformations is based on the observed increase in affinity of the heavy chain for β_2m upon peptide binding and the biexponential kinetics of peptide dissociation. Moreover this notion is in agreement with results of time-resolved intrinsic tryptophan fluorescence measurements of the single-chain H-2K^d (SC$^-$2K^d) and H-2K^d and their peptide complex (Dittes et al., 1994; Gakamsky et al., 1996). The multiple tryptophan residues in the K^d molecules enables a nonradiative energy transfer among them which affects its fluorescence pattern (Gakamsky et al., 1995). A comparison between the energy transfer among tryptophan residues in the heterodimer and in its complex with NP21 shows that it is more efficient in the ternary complex. Since six of the tryptophans are in the vicinity of the binding groove and the energy transfer is a function of separation distances between the donor and acceptor and their orientations, we concluded that peptide binding induced a conformational change in the molecule. From analysis of the energy transfer kinetics, we further concluded that the structural changes occurred at least proximal to the binding groove terminals.

It is interesting to note that the maximum of the dansyl emission of the least stable complexes (i.e., dNP1 and dNP21) is shifted to 490 nm, whereas those of the other complexes were at about 525 nm. It is well known that the position of the emission maximum of dansyl molecule correlates with polarity of its microenvironment: the shorter the wavelength of the dye's emission, the lower its environment's polarity. Therefore, the dansyl group of dNP1 and dNP21 becomes less exposed to water upon H-2K^d binding. The low affinity of dNP1 was expected since structural studies have shown that peptide's N-terminal amino group is hydrogen bonded to the site (Latron et al., 1992; Madden et al., 1991). Dansylation of this amino group obviously prevents that interaction and hence reduces the affinity. The low affinity of dNP21 was unexpected and is most probably a result of the dansyl perturbing the fit into the H-2K^d binding groove. The pronounced blue shift of the dansyl's emission maximum clearly suggests that it is screened from water, but optimal binding interactions into the groove are apparently compromised.

The above reaction scheme explains the β_2m concentration dependence of the equilibrium titration results. Equilibrium titrations of an unstable binding site cannot be depicted by a simple bimolecular reaction where the saturation binding term in the Scatchard plot coordinates yields the equilibrium dissociation constant. Due to the limited stability of the heterodimer, the ternary complex assembly kinetics are biexponential and proceed either by peptide binding to the heterodimer with a time constant τ_2 or as assembly from three separated components with a time constant τ_1. In the studied cases these two time constants differ by about 2 orders of magnitude. The contributions of these two processes is determined by the concentrations of the heterodimer, its constituents, and the peptide. Excess of β_2m shifts the equilibrium to produce the heterodimer and decreases concentration of the dissociated heavy chains. Therefore, the lower the dissociated fraction, the more the reaction corresponds to the bimolecular scheme and the

closer is the Scatchard plot to a linear function. Under this experimental condition, the average assembly rate constant, k_{on}, approximates the rate constant of the peptide binding to the heterodimer, k_2, and the peptide equilibrium dissociation constant, K_d, calculated as the slope of the Scatchard plot, becomes closer to the ratio of dissociation to association rate constants.

The three interacting components of H-2K^d−peptide are an example of a system operating under allosteric control: Association of β_2m with the heavy chain promotes the final folding of α_1 domain causing the peptide binding site to attain its high-affinity conformation which promotes peptide binding. Peptide bound to the heterodimer interacts with the groove residues thereby inducing a change in conformation of the heavy chain and increasing its affinity for β_2m. This in turn shifts the complex to its stable ternary conformation. In contrast, peptide dissociation shifts the heterodimer back to its low-affinity conformation which results in β_2m dissociation. Thus, we hypothesize that the noncovalent association of β_2m with the heavy chain and the lack of disulfide bridge in the α_1 domain are structural elements yielding a positive feedback in the ternary complex assembly. This feature of the class I MHC molecules is rationalized by its functional requirements: Peptide structure determines the ternary complex lifetime, and peptide rebinding to class I molecule on the cell surface is rendered unlikely by the instability of empty heterodimers and the low peptide affinity of the isolated heavy chains. Therefore the limited stability of the heterodimer controlled by the above allosteric mechanism has an important immunological significance.

The direct experimentally resolved observation of the peptide binding process to the class I MHC heterodimer and elucidation of the role of β_2m in the complex assembly reported here were attained by the application of nonradiative energy transfer for monitoring the ternary complex formation. We found that the peptide binding rate constants are about 5 orders of magnitude higher than those measured for H-2L^d by spun-column gel filtration (10 M^{-1} s^{-1}) (Boyd et al., 1992) and 2 orders of magnitude faster than those determined by the fluorescence binding assay for the SC-2K^d (1.14×10^3 M^{-1} s^{-1}) (Ojcius et al., 1993). The marked differences between values reported here and that determined by Boyd et al. could be due to the limited time resolution of the employed method. A possible reason of discrepancy between the peptide binding rate constant to the SC-K^d and H-2K^d molecules may lie in structural constrains imposed by the covalent linkage within the SC-K^d.

The resolution provided by the present method enables a detailed quantitative examination of the nature of the peptide−H-2K^d interactions, specifically how the peptide dissociation rate constants determine the affinity of different peptides. To further deepen our understanding of the complex assembly mechanism, it would be important to investigate how the peptide's termini and side chains' interactions with the binding groove stabilize the conformation of the ternary complex. Are the same atomic contacts between peptide and the heavy chain responsible for this binding and for the transition of the heavy chain to its stable conformation? To this end it is important to clarify the mechanism of the complex dissociation: whether fluctuations in the interface between the heavy chain and β_2m induce the peptide dissociation from the ternary complex or the peptide dissociation induces the heavy chain conformational transition and hence β_2m dssociation.

ACKNOWLEDGMENT

We thank Ms. J. Johnson for production and purification of the recombinant H-2K^d molecules, Dr. Y. Shai for HPLC peptide purification, and Mr. A. Licht for technical assistance. We are greatly indebted to Dr. A. A. Goldin for generously providing the Global Analysis program.

REFERENCES

Boyd, L. F., Kozlowski, S., & Margulies, D. H. (1992) *Proc. Natl. Acad. Sci. U.S.A. 89*, 2242−2246.
Catipovic, B., Talluri, G., Oh, J., Wei, T., Su, X. M., Johansen, T. E., Edidin, M., & Schneck, J. P. (1994) *J. Exp. Med. 180*, 1753−1761.
Cerundolo, V., Elliott, T., Elvin, J., Bastin, J., Rammensee, H. G., & Townsend, A. (1991) *Eur. J. Immunol. 21*, 2069−2075.
Dittes, K., Gakamsky, D. M., Haran, G., Haas, E., Ojcius, D. M., Kourilsky, P., & Pecht, I. (1994) *Immunol. Lett. 40*, 125−132.
Elliott, T., Vincenzo, C., Elvin, J., & Townsend, A. (1991) *Nature 351*, 402−406.
Engelhard, V. H. (1994) *Curr. Opin. Immunol. 6*, 13−24.
Engelhard, V. H., Appella, E., Benjamin, D. C., Bodnar, W. M., Cox, A. L., Chen, Y., Henderson, R. A., Huczko, E. L., Michel, H., Sakaguchi, K., et al. (1993) *Chem. Immunol. 57*, 39−62.
Fahnestock, M. L., Tamir, I., Narhi, L., & Bjorkman, P. J. (1992) *Science 258*, 1658−1662.
Fahnestock, M. L., Johnson, R. M., Feldman, R., Tsomides, T. J., Mayer, J., Narhi, L. O., & Bjorkman, P. J. (1994) *Biochemistry 33*, 8149−8158.
Falk, K., Rotzschke, O., Deres, K., Metzger, J., Jung, G., & Rammensee, H. G. (1991) *J. Exp. Med. 174*, 425−434.
Gakamsky, D. M., Haas, E., Robbins, P., Strominger, J. L., & Pecht, I. (1995) *Immunol. Lett. 44*, 195−201.
Gakamsky, D. M., Bjorkman, P. J., Haas, E., & Pecht, I. (1996) (to be published).
Hunt, D. F., Henderson, R. A., Shabanowitz, J., Sakaguchi, K., Michel, H., Sevilir, N., Cox, A., Appella, E., & Engelhard, V. H. (1992) *Science 255*, 1261−1263.
Latron, F., Pazmany, L., Morrison, J., Moots, J., Saper, M. A., McMichael, A., & Strominger, J. L. (1992) *Science 257*, 964−967.
Madden, D. R. (1995) *Annu. Rev. Immunol. 13*, 587−622.
Madden, D. R., Gorga, J. C., Strominger, J. L., & Wiley, D. C. (1991) *Nature 353*, 321−325.
Madden, D. R., Garboczi, D. N., & Wiley, D. C. (1993) *Cell 75*, 693−708.
Matsumura, M., Saito, Y., Jackson, M. R., Song, E. S., & Peterson, P. A. (1992) *J. Biol. Chem. 267*, 23589−23595.
Ojcius, D. M., Godeau, F., Abastado, J. P., Casanova, J. L., & Kurilsky, P. (1993) *Eur. J. Immunol. 23*, 1118−1124.
Olsen, A. C., Pedersen, L. O., Hansen, A. S., Nissen, M. H., Olsen, M., Hansen, P. R., Holm, A., & Buus, S. (1994) *Eur. J. Immunol. 24*, 385−392.
Parker, C. A. (1968) *Photoluminescence of solutions*, Elsever, Amsterdam.
Parker, K. C., DiBrino, M., Hull, L., & Coligan, J. E. (1992) *J. Immunol. 149*, 1896−1904.
Pecht, I., Maron, E., Arnon, R., & Sela, M. (1971) *Eur. J. Biochem. 19*, 368−371.
Rock, K. L., Gamble, S., Rothstein, L., Gramm, C., & Benacerraf, B. (1991) *Cell 65*, 610−620.
Romero, P., Corradin, G., Luescher, I. F., & Maryanski, J. L. (1991) *J. Exp. Med. 174*, 603−612.
Rotzschke, O., Falk, K., Deres, K., Schild, H., Norda, M., Metzger, J., Jung, G., & Rammensee, H. G. (1990) *Nature 348*, 252−254.
Smith, J. D., Solheim, J. C., Carreno, B. M., & Hansen, T. H. (1994) *Mol. Immunol. 32*, 531−540.
Solheim, J. C., Carreno, B. M., Myers, N. B., Lee, D. R., & Hansen, T. H. (1995) *J. Immunol. 154*, 1188−1197.
Stern, L. J., & Wiley, D. C. (1994) *Structure 15*, 245−251.
Wetlaufer, D. B. (1962) *Adv. Protein Chem. 17*, 33−390.
Zhang, W., Young, A. C. M., Imarai, M., & Nathenson, S. G. (1992) *Proc. Natl. Acad. Sci. U.S.A. 89*, 8403−8407.

BI961707U